Scuola di Dottorato in Ingegneria Leonardo da Vinci – a.a. 2009/10

PROPRIETÀ MECCANICHE, OTTICHE, ELETTRONICHE DEI MATERIALI ALLE PICCOLE E PICCOLISSIME SCALE

Versione 1 – Ottobre 2010 – http://www.df.unipi.it/~fuso/dida

Parte 7
Proprietà ottiche dei materiali semiconduttori: dalla scale macroscopiche alle scale piccolissime (incluse applicazioni!)

Me 13.10 13-16 aula S1 DF

Outlook

- How to approach the optical properties in the (or semiclassical) terms:
  Photons and quantized matter (e.g., the hydrogen atom)
- Short resume on the electronic properties of (bulk) materials:
  Metals vs Dielectrics (Semiconductors)
- Qualitative behavior of the material electrons upon optical excitation:
  Optical transitions in semiconductors
- The optical properties of semiconductors and their exploitations in optoelectronics
- The need for small dimensions and the principle of operation of laser diodes
- Beyond optoelectronics: the example of quantum dots as markers in biological tissues

Back to quantum physics: photons and matter

$$E^2 = p^2c^2 + m^2c^4.$$

The energy and momentum of a photon depend only on its frequency (ν) or inversely, its wavelength (λ):

$$E = \hbar\omega = h\nu = \frac{hc}{\lambda}$$

$$\mathbf{p} = \hbar\mathbf{k},$$

Photons as quanta of the radiation energy

where $\mathbf{k}$ is the wave vector (where the wave number $k = |\mathbf{k}| = 2\pi/\lambda$), $\omega = 2\pi\nu$ is the angular frequency, and $\hbar = h/2\pi$ is the reduced Planck constant.[14]

Since $\mathbf{p}$ points in the direction of the photon's propagation, the magnitude of the momentum is

$$p = \hbar k = \frac{h\nu}{c} = \frac{h}{\lambda}.$$

The photon also carries spin angular momentum that does not depend on its frequency.[15] The magnitude of its spin is $\sqrt{2}\hbar$ and the component measured along its direction of motion, its helicity, must be $\pm\hbar$. These two possible helicities, called right-handed and left-handed, correspond to the two possible circular polarization states of the photon.[16]

Bohr postulate: $L = mvr = n\frac{h}{2\pi}$

Matter as a quantized system

Quantization of radius: $r_n = \frac{n^2 h^2 \varepsilon_o}{\pi m Z e^2}$

Quantization of energy: $E_n = -\frac{mZ^2e^4}{8\varepsilon_o^2 h^2}\frac{1}{n^2}$ $\quad E_n = -13.6\frac{Z^2}{n^2}\ eV$

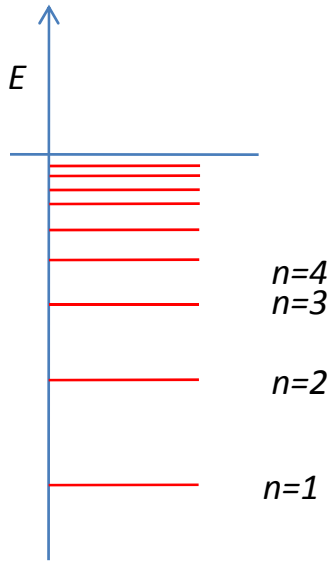

Back to quantum physics: optical interaction with a single atom

Discrete energy levels

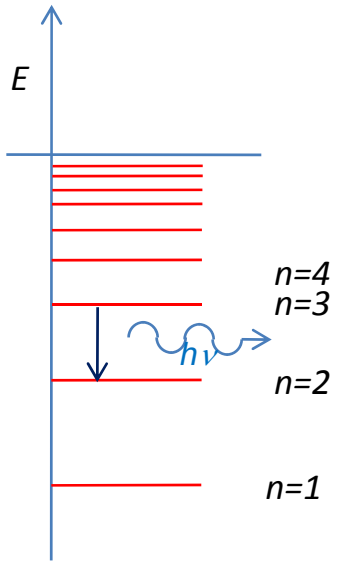

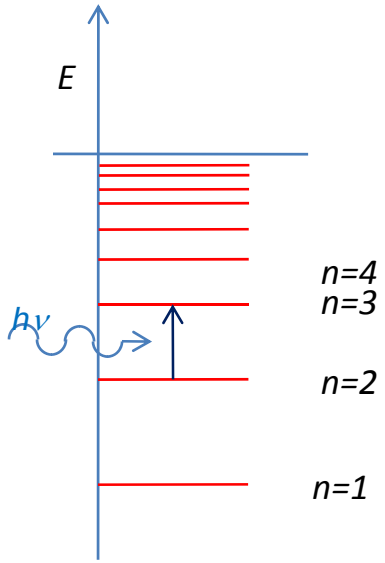

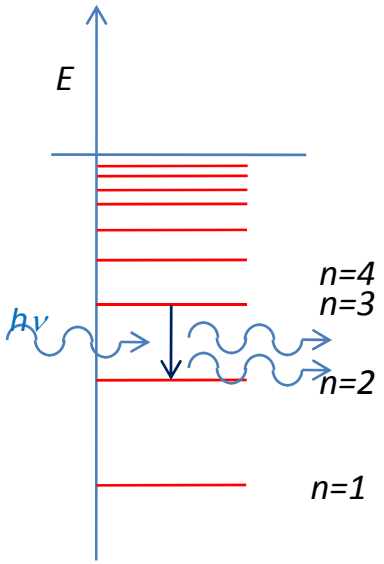

Spontaneous decay

Absorption

Stimulated emission

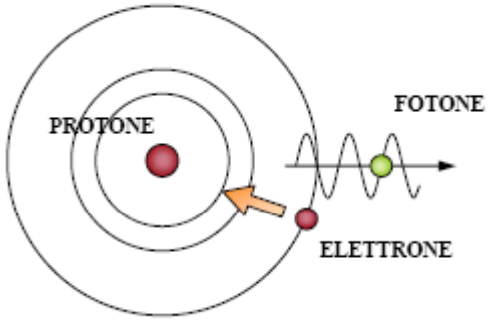

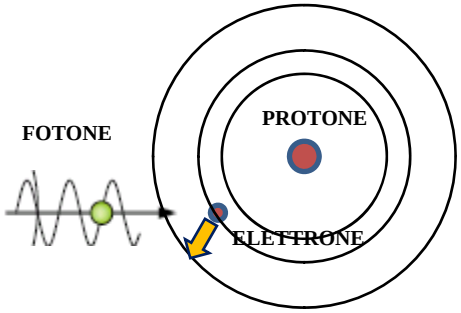

Energy balance:

$h\nu = -(E_{fin}-E_{in})$

Moreover: impulse and angular momentum must be conserved, too

Back to quantum physics: how to describe a solid state system

Un modello elementare descrive un solido come l'insieme di un gran numero di ioni disposti in maniera regolare (cristallo) tra i quali si muovono liberamente gli elettroni di valenza, che non interagiscono nè con gli ioni, nè tra loro, ma sono vincolati solo dalle dimensioni finite del solido e dalle conseguenze energetiche del rispetto del principio di esclusione di Pauli.

Tale modello "a elettroni liberi" nella sua semplicità descrive il comportamento ottico di alcuni metalli (riflettività nel visibile e assorbimento nell'UV), ma per la stragrande maggioranza dei materiali va corretto prendendo in considerazione l'effetto del potenziale elettrostatico degli ioni.

Tra tutti gli elettroni del solido, alcuni non risentono molto di tale potenziale e si comportano come elettroni liberi, altri invece sentono in modo particolare il potenziale con la periodicità del reticolo reale, e si vede che l'elettrone può oscillare in due modi diversi mantenendo lo stesso passo dell'onda: in un modo ha più probabilità di trovarsi centrato sullo ione, dove trova un potenziale molto elettronegativo, ed ha più energia (stato "*s*" di antilegame); nell'altro modo ha più probabilità di trovarsi vincolato nella posizione intermedia tra i due ioni (contribuendo a tenerli uniti) e perde energia (stato "*p*" di legame).

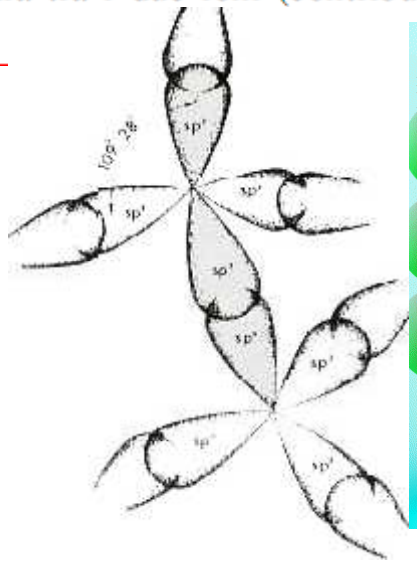

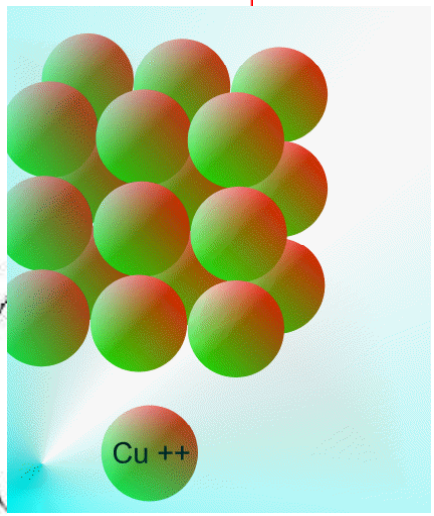

We saw the "ion" behavior (e.g., phonons)

We now move to "electrons"

http://www.dsm.unisalento.it/webutenti/massimo.digiulio/public/ProprOttiche06.pdf

Back to quantum physics: the electronic wavefunction

Single atom: quantum system (discrete energy levels) → Biatomic molecule (manifold of levels) → solid (energy bands)

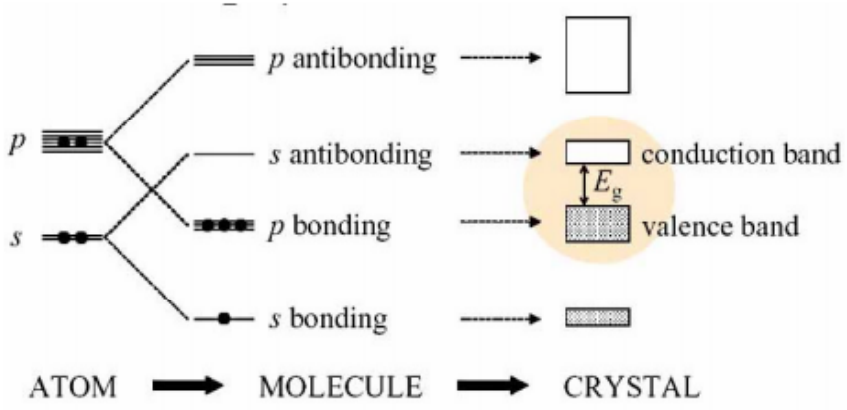

- Four valence electrons per atom: Group IV (C, Si, Ge),
- III-V compounds (GaAs, InAs, InSb, GaN ….)
- II-VI compounds (ZnS, ZnSe, CdSe, HgTe, ….)
- V.B. → C.B. is $p \rightarrow s$, hence allowed transition

A sinistra sono rappresentati gli orbitali atomici s e p che, sempre nel caso del Si, sono quelli di valenza, cioè quelli degli elettroni più esterni (il Si ha valenza 4).

Nel momento in cui si volesse formare una molecola (cioè mettere insieme solo due o quattro di questi atomi), per il fatto che gli elettroni possono stare solo o sull'atomo o tra i due atomi, si creano degli orbitali molecolari di legame e di antilegame, che a loro volta possono essere occupati o meno.

Ognuno di questi due stati dovrebbe avere lo stesso valore di energia per tutti gli elettroni di valenza degli atomi che formano il solido, ma per il Principio di Esclusione di Pauli (che non consente a due elettroni che si trovino nello stesso spazio di avere esattamente la stessa energia, a parte la differenza di spin) questo non può avvenire: ogni elettrone varia di pochissimo la sua energia (e il suo vettore d'onda **k** con cui viene descritto in Meccanica Quantistica) in modo da obbedire al principio e tutti i valori così ottenuti, molto vicini fra loro, coprono un intervallo detto "banda", una per lo stato "s" e una per lo stato "p" (le bande possono essere più di due se il numero di elettroni di valenza è grande). La variazione di k è inversamente proporzionale alle dimensioni macroscopiche del solido ("L"). Il numero di stati **in ciascuna banda** è pari al numero di atomi nel solido, moltiplicato per 2 per il diverso spin.

Classification of matter from the electronic point of view

METALLI / SEMICONDUTTORI / ISOLANTI

Le bande di energia sono quindi costituite da stati elettronici, che sono però definiti indipendentemente dal fatto se essi siano effettivamente occupati o meno dagli elettroni. Bisogna quindi distinguere i concetti di STATO ENERGETICO e STATO dell'ELETTRONE: gli stati energetici possibili ai vari valori di energia sono "contati" da una funzione detta "densità di stati", ma non è detto che siano tutti occupati dagli elettroni (si riempiranno prima quelli ad energia più bassa e rimarranno livelli vuoti). L'occupazione dei vari livelli delle bande dipende da numerosi fattori:

1) numero di elettroni di valenza da "sistemare",

2) temperatura

3) andamento dell'energia delle bande in funzione di k ("forma" delle bande) e quindi valore di E_g.

Ricordando che per ogni livello energetico possibile ci possono essere due elettroni, purchè abbiano spin opposto, allora, detto N il numero totale di atomi del solido, possiamo stabilire questa regola **di massima**:

- se il numero di elettroni di valenza è pari, alcune bande si riempiono completamente e le altre restano completamente vuote (ad esempio con valenza 2 abbiamo in una banda $2 \times N$ stati (il 2 è dovuto allo spin) e proprio $2 \times N$ elettroni da mettere; con valenza 4 abbiamo in due bande $2 \times (2 \times N)$ stati e proprio $4 \times N$ elettroni da mettere). Non essendoci alcun livello non occupato in nessuna banda piena non è possibile nessun cambiamento di stato **k** per gli elettroni, nemmeno sotto l'azione di una campo elettrico anche intenso: questo è il comportamento dei MATERIALI ISOLANTI;
- quando invece un atomo ha un numero dispari di elettroni di valenza una banda sarà mezza piena e mezza vuota (ad esempio con valenza 1 abbiamo in una banda $2 \times N$ stati disponibili, ma solo N elettroni; con valenza 3 abbiamo in due bande $2 \times (2 \times N)$ stati e $3 \times N$ elettroni da mettere); rimarranno quindi degli stati disponibili, non occupati da elettroni, ma pur sempre nella stessa banda, e perciò facilmente raggiungibili dagli elettroni stessi con solo una piccola variazione di energia, come quella fornita da un campo elettrico anche debole: questo è il comportamento dei MATERIALI METALLICI.

Optical transitions in semiconductors

Dal punto di vista ottico, indipendentemente dalla temperatura la transizione energetica di elettroni dalla banda di valenza a quella di conduzione avviene facilmente se il solido riceve ed assorbe fotoni di energia hν almeno pari a E_g.

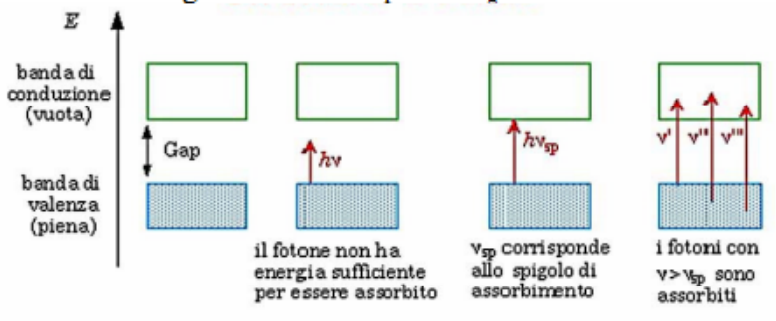

Questa possibilità è la base delle proprietà ottiche dei semiconduttori e degli isolanti: quando viene assorbito un fotone di energia **almeno** pari a questo salto, l'elettrone riesce a fare la transizione.

Tenere sempre presente che la relazione tra energia hν espressa in eV e lunghezza d'onda espressa in nm è

$$E = h\nu\ (eV) = 1240 / \lambda\ (nm)$$

(radiazione visibile: λ = 400-700 nm → *E* ~ 1.5-3 eV)

Cristallo	Eg (eV)
Diamante	5.4
Si	1.14
Ge	0.67
InN	0.7
InP	1.34
InSb	0.17
InAs	0.33
GaAs	1.43
GaN	3.37
GaP	2.3
SiC	3
Al_2O_3	5.7
AlAs	2.16
PbS	0.37
CdS	2.42
HgTe	0.15
ZnO	3.2
ZnS	3.6
AgCl	3.2
AgI	2.8
Cu_2O	2.1
NaCl	7.2

Qualitatively: light is absorbed by a semiconductor if photon energy is larger than the band gap

(in dielectrics, photon energy is so large that radiation in the UV range is needed)

Otherwise: in principle the material is transparent (obviosuly, reflection at the interface can occur as well)

Technology: optolelectronics

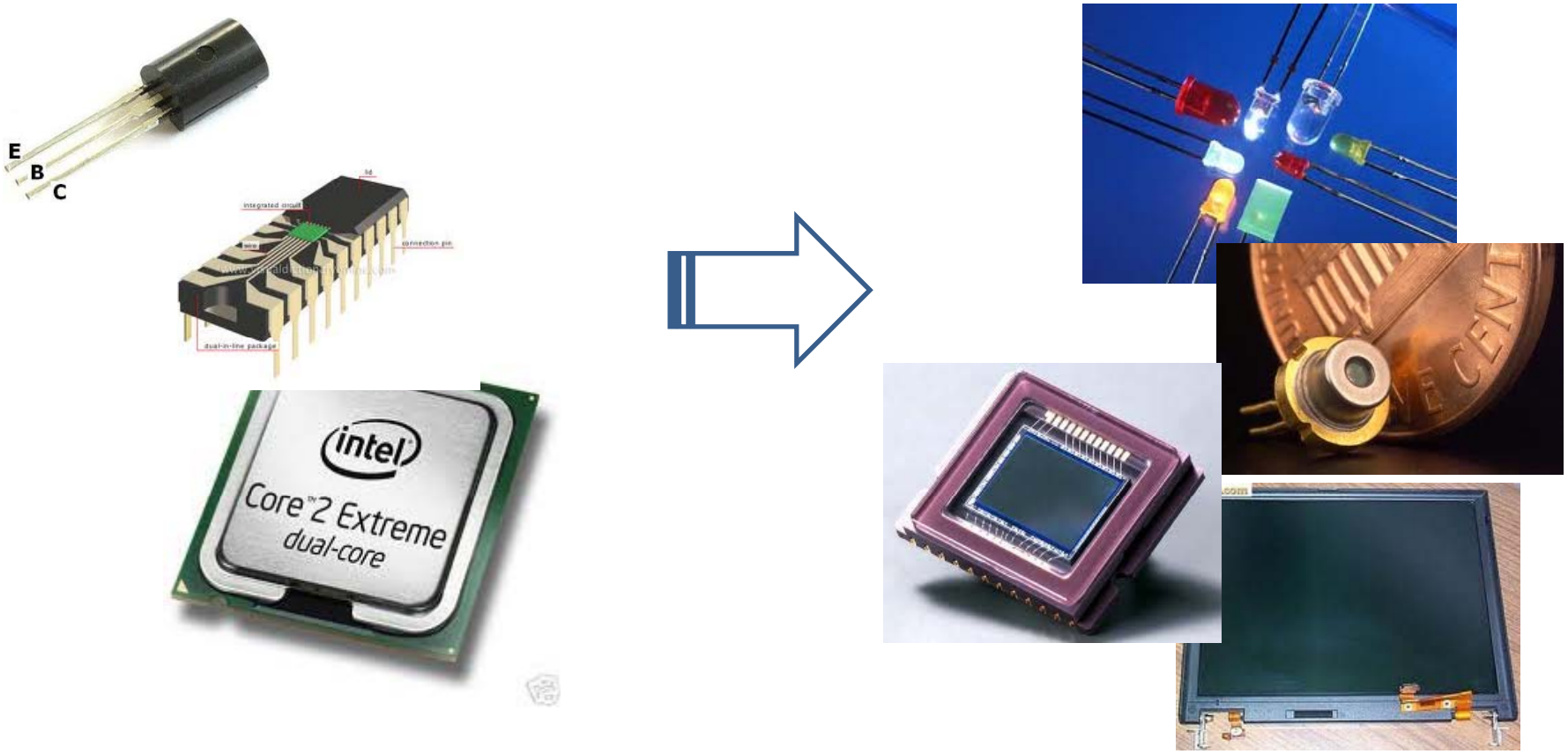

Semiconductors (especially Silicon) are the buiding blocks of electronics

Technology has been greatly interested in optoelectronics (e.g., detectors, sources)

The real world: Silicon and its (unhappy) properties

Broad diffusion of optoelectronics driven by the availability of solid-state active media, but (bulk) semiconductors, e.g., Si, are not suited because of energy gap (in the IR) and indirect transitions

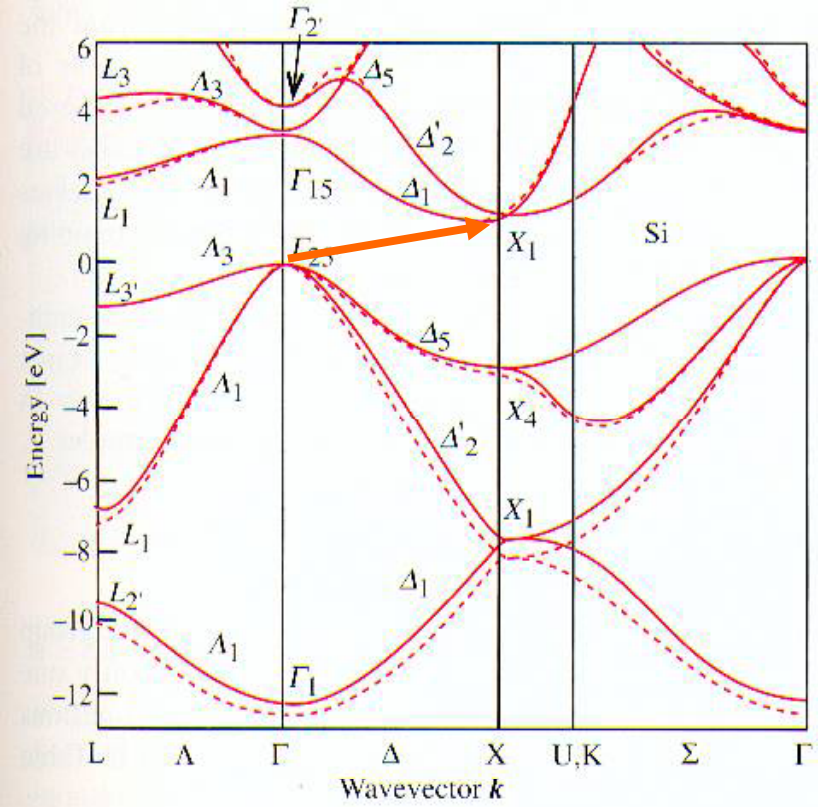

Fig. 2.10. Electronic band structure of Si calculated by the pseudopotential technique. The *solid* and the *doted lines* represent calculations with a **nonlocal** and a **local pseudopotential**, respectively. [Ref. 2.6, p. 81]

Band structure of Si (determined by its crystal structure)

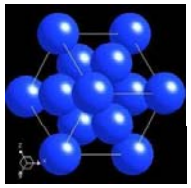

The top of valence band and the bottom of the conduction band are displaced each other

⇩

Momentum conservation implies phonons to be involved in the absorption process

⇩

Transition probability is small (10^{-5}-10^{-6} s^{-1}) (and wavelength is in the IR, above 1 μm)

Bulk semiconductive materials can be hardly used in optoelectronics devices

Da Yu and Cardona
Fundamentals of Semicond.
Springer (1996)

What's the meaning of small, here

Optics (in the visible, $\lambda \approx 400–700$ nm)
vs nanotechnology (dimensions typ. < 100 nm)
***Different dimensional scales*!!**

But:

-Semiconductive nanostructures (e.g., MQW, QD) are essential for providing peculiar optical features exploited, for instance, in diode lasers

- Nanosized metal structures exhibit peculiar optical response (e.g., plasmon resonances)

- Nanostructured materials can "manipulate" radiation (e.g., photonic band gaps, *near-field optics (we'll see something later!)*

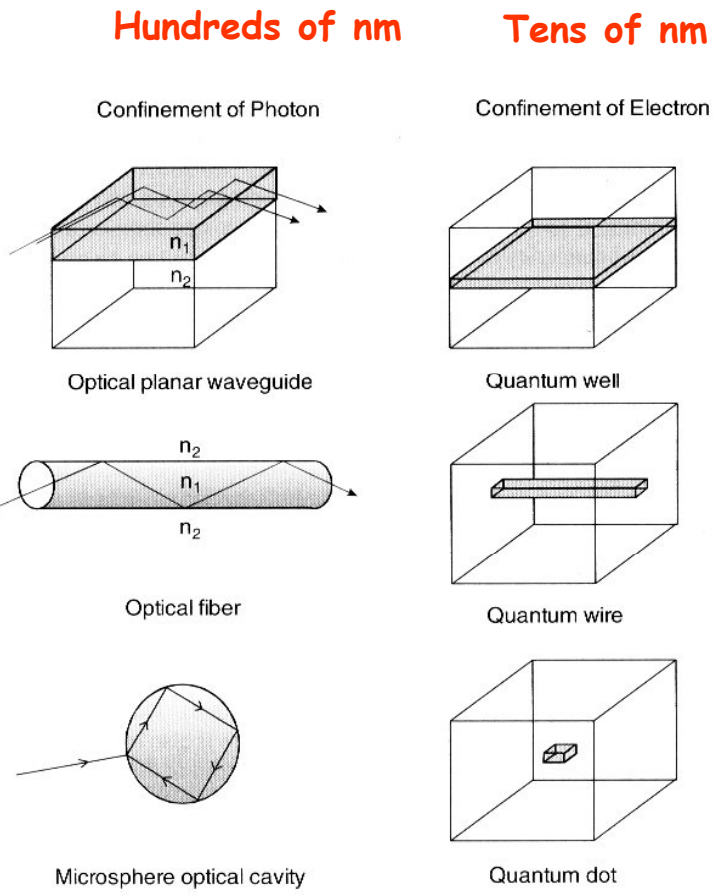

Figure 2.2. Confinements of photons and electrons in various dimensions and the configurations used for them. The propagation direction is *z*.

Da P.N. Prasad,
Nanophotonics,
Wiley (2004)

Great (and partially new) interest on optics and small or even ultra-small systems

Matter and waves

Remember: according to the matter/wave duality and the de Broglie principle a free particle with ***p*** impulse can be described by a wavefunction , independently on whether a photon or a massive particle is concerned

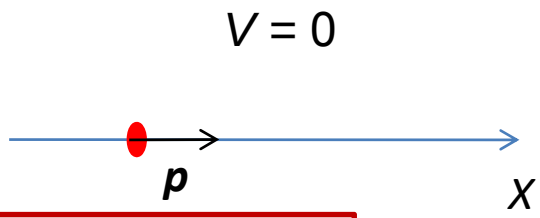

de Broglie :

$$\Psi(x,t) \propto e^{ikx} e^{-i\omega t} = \psi(x)\varphi(t)$$

$$\psi(x) = e^{ikx}$$

con $p = \hbar k$

de Broglie wavelength: $\lambda_{dB} = 2\pi/k = h/p$

The de Broglie relations

The de Broglie equations relate the wavelength λ and frequency f to the momentum p and energy E, respectively, as

$$\lambda = \frac{h}{p} \text{ and } f = \frac{E}{h}$$

where h is Planck's constant. The two equations are also written as

$$p = \hbar k$$

$$E = \hbar \omega$$

where $\hbar = h/(2\pi)$ is the reduced Planck's constant (also known as **Dirac's constant**, pronounced "h-bar"), k is the angular wavenumber, and ω is the angular frequency.

Example:
Electron, $m \sim 10^{-30}$ kg, with speed $v = 10^5$ m/s:
This corresponds to a kinetic energy $E = mv^2/2 \sim 5\times10^{-19}$ J ~ 4 eV
(i.e., an electron accelerated by a voltage $V = 5$ V!)
And to a de Broglie wavelength $\lambda_{dB} = h/(mv) \sim 6$ nm

Artificial materials grown layer by layer

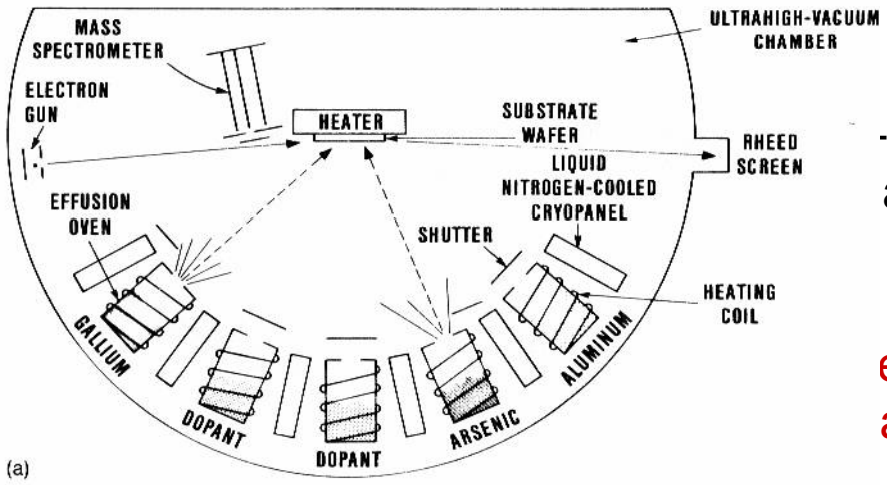

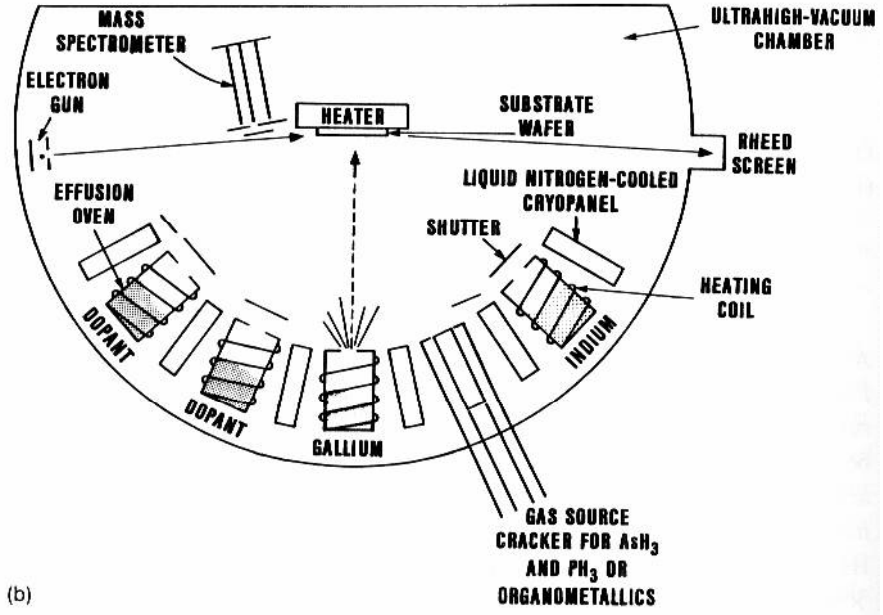

Key points for MBE:

- clean process (UHV, $p \leq 10^{-10}$mbar)
- all continuous deposition rate (~ 1 μm/h)
- suitable with semiconductor

ess easily controlled at the monolayer level

atively) low kinetic energy favors epitaxy

Heterostructures easily fabricated

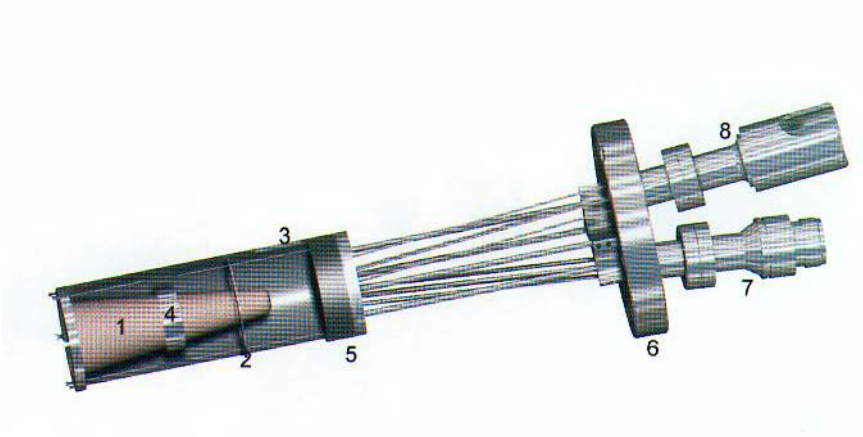

Molecular Beam Epitaxy (MBE) and its variants

Semiconductive material choice

Da Yu and Cardona
Fundamentals of Semicond.
Springer (1996)

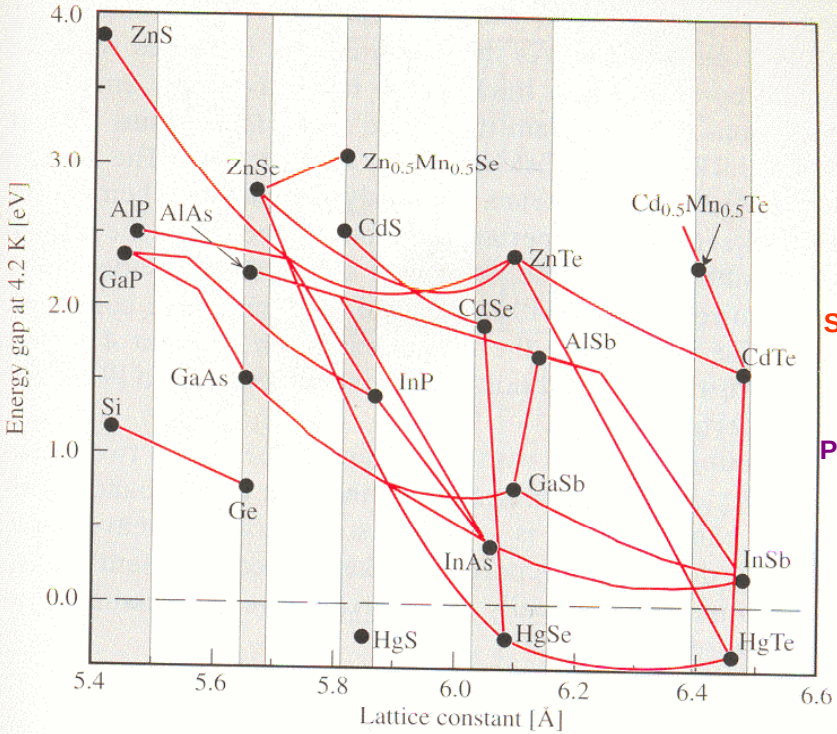

Fig. 9.2. A plot of the low temperature energy bandgaps of a number of semiconductors with the diamond and zinc-blende structure versus their lattice constants. The *shaded regions* highlight several families of semiconductors with similar lattice constants. Semiconductors joined by *solid lines* form stable alloys. [Chen A.B., Sher A.: *Semiconductor Alloys* (Plenum, New York 1995) Plate 1]

A wide choice of semiconductors is available to tune the gap in a broad range (from blue to near-IR)

Now, higher gaps achieved with GaN

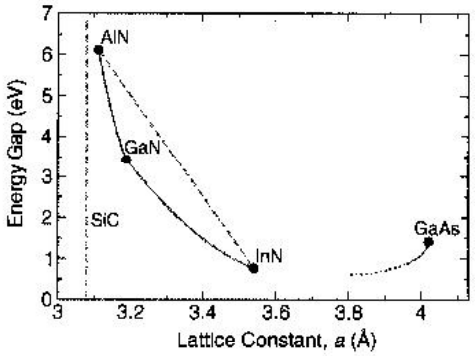

Figure 1. Fundamental bandgap versus basal-plane lattice constant of nitride materials compared with SiC and GaAs. The solid curves represent the ternary mixtures AlN/GaN,[10] GaN/InN,[11] and GaN/GaAs.[12] The dotted curve qualitatively indicates the continuation of the GaNAs gap toward GaN.

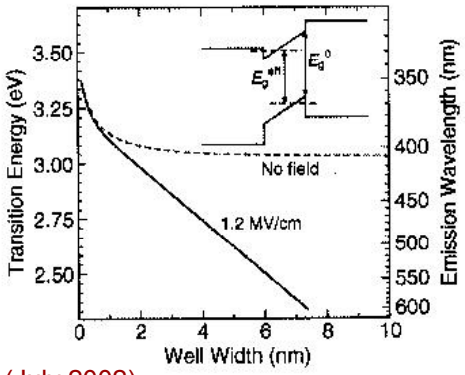

See MRS Bull. 27 (July 2002)

Figure 3. Transition energy of $Ga_{0.9}In_{0.1}N$/GaN quantum wells versus well width, with and without built-in electric field. The inset shows a schematic view of the band scheme, the effective bandgap E_g^{eff}, and the original bandgap E_g^0.

Semiconductive heterostructures

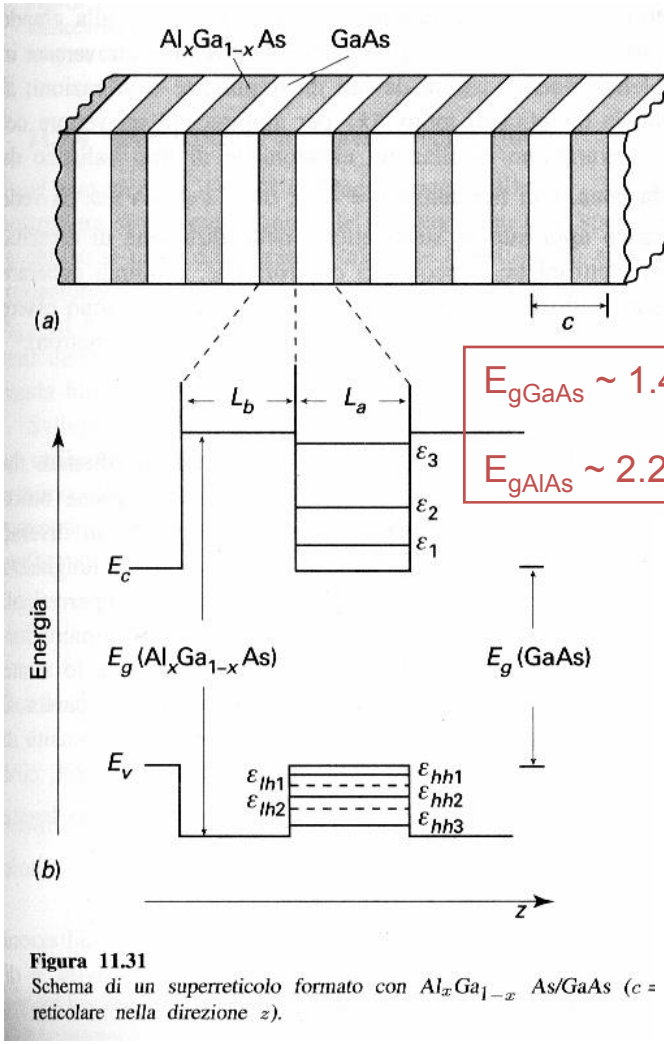

Figura 11.31
Schema di un superreticolo formato con Al_xGa_{1-x} As/GaAs (c = reticolare nella direzione z).

Heterostructures(superlattices): sequence of layers made of semiconductors with different gap energies (*as we have already seen!)*

E_{gGaAs} ~ 1.4 eV

E_{gAlAs} ~ 2.2 eV

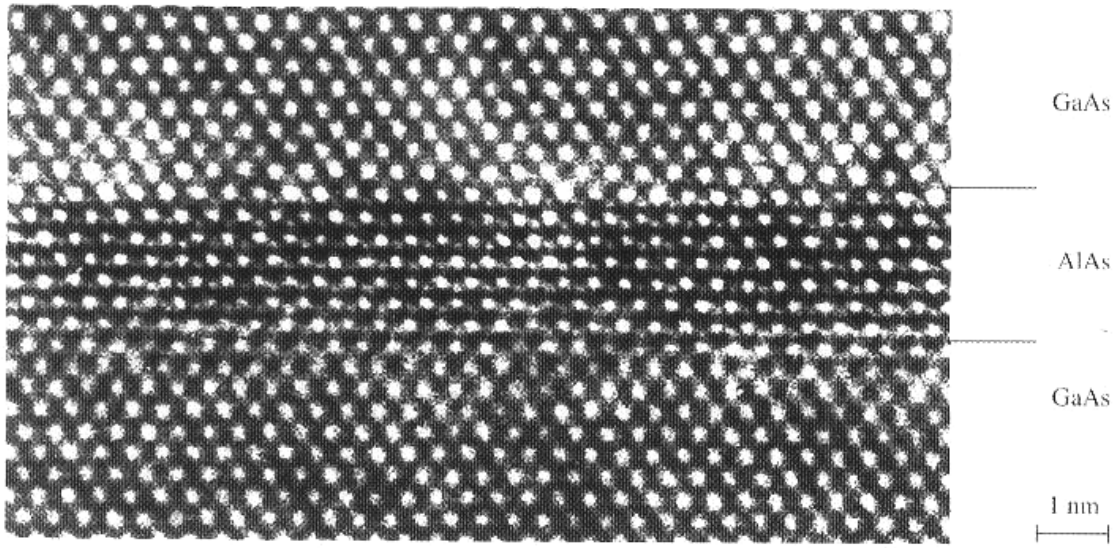

Fig. 9.1. High resolution transmission electron micrograph (TEM) showing a GaAs/AlAs superlattice for a [110] incident beam. (Courtesy of K. Ploog, Paul Drude Institute, Berlin.) In spite of the almost perfect interfaces, try to identify possible Al atoms in Ga sites and vice versa

Da Bassani Grassano,
Fisica dello Stato Solido,
Boringhieri (2000)

Quantum Well I

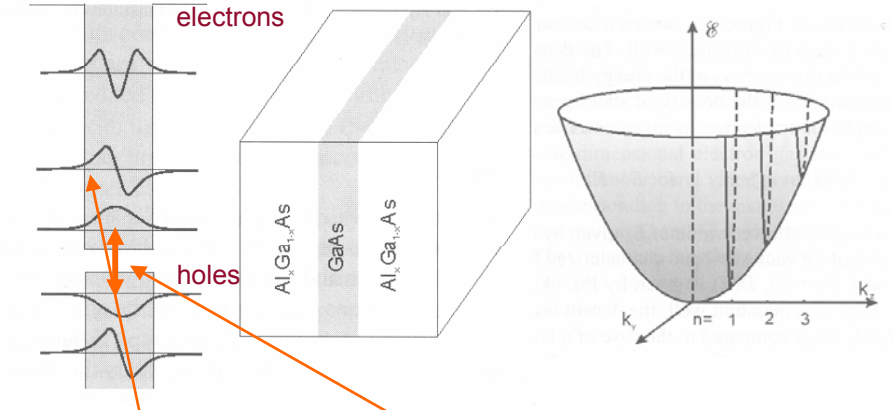

- For energies $E < V$, the energy levels of the electron are quantized for the direction z of the confinement; hence they are given by the model of particle in a one-dimensional box. The electronic energies in the other two dimensions (x and y) are not discrete and are given by the effective mass approximation discussed in Chapter 2. Therefore, for $E < V$, the energy of an electron in the conduction band is given as

$$E_{n,k_x,k_y} = E_C + \frac{n^2\hbar^2}{8m_e^* l^2} + \frac{\hbar^2(k_x^2 + k_y^2)}{2m_e^*} \qquad (4.1)$$

where $n = 1, 2, 3$ are the quantaum numbers. The second term on the right-hand side represents the quantized energy; the third term gives the kinetic energy of the electron in the x–y plane in which it is relatively free to move. The symbols used are as follows: m_e^* is the effective mass of electron, and E_C is the energy corresponding to the bottom of the conduction band.

Equation (4.1) shows that for each quantum number n, the values of wavevector components k_x and k_y form a two-dimensional band structure. However, the wavevector k_z along the confinement direction z takes on only discrete values, $k_z = n\pi/l$. Each of the bands for a specific value of n is called a sub-band. Thus n becomes a sub-band index. Figure 4.2 shows a two-dimensional plot of these sub-bands.

- For $E > V$, the energy levels of the electron are not quantized even along the z direction. Figure 4.1 shows that for the AlGaAs/GaAs quantum well, the quantized levels $n = 1$–3 exist, beyond which the electronic energy level is a continuum. The total number of discrete levels is determined by the width l of the well and the barrier height V.

- The holes behave in analogous way, except their quantized energy is inverted and the effective mass of a hole is different. Figure 4.1 also shows that for the holes, two quantized states with quantum numbers $n = 1$ and 2 exist for this particular quantum well (determined by the composition of AlGaAs and the width of the well). In the case of the GaAs system, two types of holes exist, determined by the curvature (second derivative) of the band structure. The one with a smaller effective mass is called a *light hole* (lh), and the other with a heavier effective mass is called a *heavy hole* (hh). Thus the $n = 1$ and $n = 2$ quantum states actually are each split in two, one corresponding to lh and the other to hh.
- Because of the finite value of the potential barrier ($V \neq \infty$), the wavefunctions, as shown for levels $n = 1, 2$, and 3 in the case of electrons and levels $n = 1$ and 2 in the case of holes, do not go to zero at the boundaries. They extend into the region of the wider bandgap semiconductor, decaying exponentially into this region. This electron leakage behavior has already been discussed in Section 2.1.3 of Chapter 2.
- The lowest-energy band-to-band optical transition (called the interband transition) is no longer at E_g, the energy gap of the smaller bandgap semiconductor, GaAs in this case. It is at a higher energy corresponding to the difference between the lowest energy state ($n = 1$) of the electrons in the conduction band and the corresponding state of the holes in the valence band. The effective bandgap for a quantum well is defined as

$$E_g^{\text{eff}} = (E_C - E_V) + \frac{h^2}{8l^2}\left(\frac{1}{m_e^*} + \frac{1}{m_h^*}\right) \qquad (4.2)$$

In addition, there is an excitonic transition below the band-to-band transition. These transitions are modifications of the corresponding transitions found for a bulk semiconductor. In addition to the interband transitions, new transitions between the different sub-bands (corresponding to different n values) within the conduction band can occur. These new transitions, called intraband or inter-sub-band transitions, find important technologic applications such as in quantum cascade lasers. The optical transitions in quantum-confined structures are further discussed in the next section.

Da P.N. Prasad,
Nanophotonics,
Wiley (2004)

Dimensionality and density of states (DOS)

Quantum confinement effects expected whenever boundary conditions are imposed by the size of the system

DOS and dimensionality

$$g(p)\,dp \propto \begin{cases} L/h\,dp & \text{1-D} \\ S/h^2\,2\pi p\,dp & \text{2-D} \\ V/h^3\,4\pi p^2\,dp & \text{3-D} \end{cases}$$

$$g(E)\,dE \propto \begin{cases} dE/\sqrt{E} & \text{1-D} \\ dE & \text{2-D} \\ \sqrt{E}\,dE & \text{3-D} \end{cases}$$

DOS expression as a function of energy turns affected by dimensionality

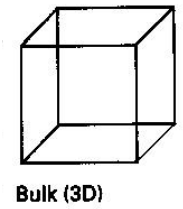

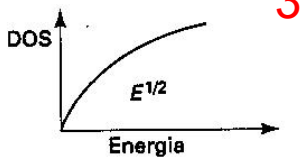

3DEG

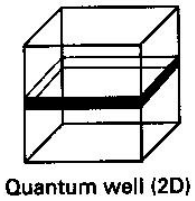

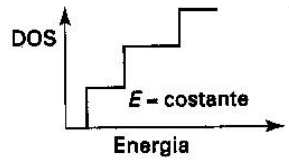

2DEG

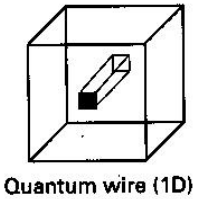

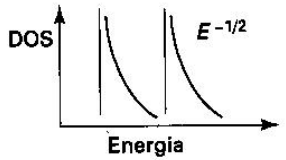

1DEG

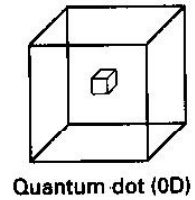

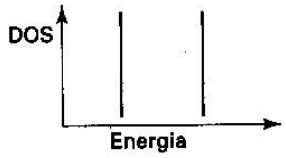

0DEG

Quantum Well II

- Another major modification, introduced by quantum confinement, is in the density of states. The density of states $D(E)$, defined by the number of energy states between energy E and $E + dE$, is determined by the derivative $dn(E)/dE$. For a bulk semiconductor, the density of states $D(E)$ is given by $E^{1/2}$. For electrons in a bulk semiconductor, $D(E)$ is zero at the bottom of the conduction band and increases as the energy of the electron in the conduction band increases. A similar behavior is exhibited by the hole, for which the energy dispersion (valence band) is inverted. Hence, as the energy is moved below the valence band maximum, the hole density of states increases as $E^{1/2}$. This behavior is shown in Figure 4.3, which also compares the density of states for electrons (holes) in a quantum well. The density of states is a step function because of the discreteness of the energy levels along the z direction (confinement direction). Thus the density of states per unit volume for each sub-band, for example for an electron, is given as a rise in steps of

$$D(E) = m_e^*/\pi^2 \qquad \text{for } E > E_1 \tag{4.3}$$

The steps in $D(E)$ occur at each allowed value of E_n given by Equation (4.1), for k_x and $k_y = 0$, then stay constant for each sub-band characterized by a specific n (or k_z). For the first sub-band with $E_n = E_1$, $D(E)$ is given by Eq. (4.3). This step-like behavior of $D(E)$ implies that for a quantum well, the density of states in the vicinity of the bandgap is relatively large compared to the case of a bulk semiconductor for which $D(E)$ vanishes. As is discussed below, a major manifestation of this modification of the density of states is in the strength of optical transition. A major factor in the expression for the strength of optical transition (often defined as the oscillator strength) is the density of states. Hence, the oscillator strength in the vicinity of the bandgap is considerably enhanced for a quantum well compared to a bulk semiconductor. This enhanced oscillator strength is particularly important in obtaining laser action in quantum wells, as discussed in Section 4.4.

DOS

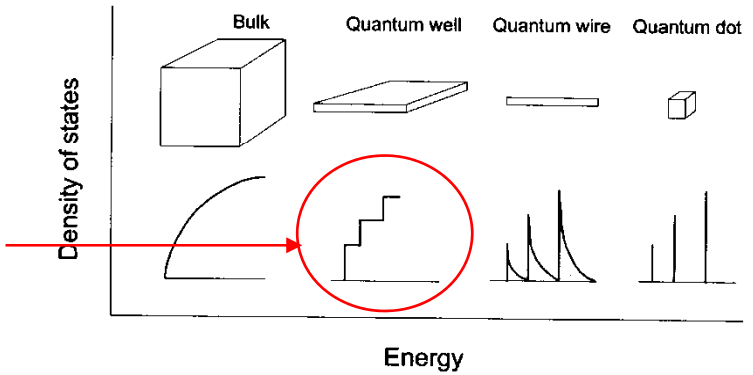

Figure 4.3. Density of states for electrons in bulk conduction band together with those in various confined geometries.

Optical transitions in quantum confined systems

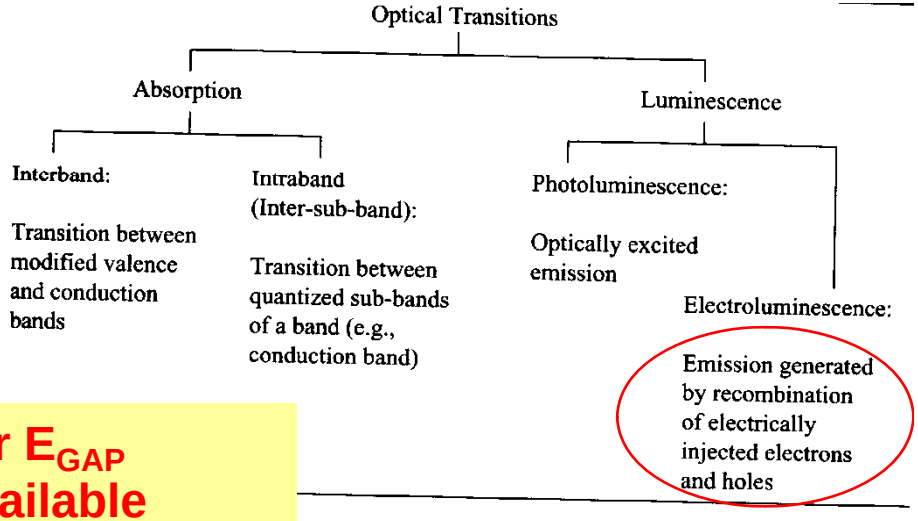

✓Interband transition energy is no longer E_{GAP}
✓Intraband (intersubband) transitions available
✓Increased transition "strength" (oscillator strength)

Excitons (a few words)

Whenever electron and hole wavefunctions overlap each other, a quasi-bound system can be formed called **exciton**

In (type I) quantum wells there is a high probability of exciton formation due to confinement of electrons and holes in the same layer

Il calcolo dell'energia di legame degli eccitoni può essere effettuato in modo analogo a quello delle impurezze nei semiconduttori se le bande di valenza e di conduzione sono sferiche e non degeneri. Analogamente a quanto visto nel cap. 11, si ricava che i livelli idrogenoidi (riferiti alla cima della banda di valenza) hanno energie date da:

Hydrogen-like energy levels!

$$E_n = E_g - \frac{\mu e^4}{2\hbar^2 \varepsilon^2} \frac{1}{n^2}, \qquad (12.107)$$

ove n è il numero quantico principale, ε la costante dielettrica, e μ la massa ridotta del complesso elettrone-buca

$$\frac{1}{\mu} = \frac{1}{m_e^*} + \frac{1}{m_h^*} \cdot \qquad (12.108)$$

Nei semiconduttori abbiamo visto che $\varepsilon \simeq 10$ e $\mu \simeq 0.5 m_e$, per cui l'energia di legame degli eccitoni sarà dell'ordine di qualche decina di meV. A causa della grande costante dielettrica l'eccitone è dunque debolmente legato e la distanza media elettrone-buca è dell'ordine di decine di distanze reticolari. Un eccitone con queste caratteristiche è chiamato eccitone di Wannier-Mott, e ne discuteremo

Electron and hole system bound by Coulomb forces

⇩

Exciton behaves like an hydrogen atom (but for some degeneracy removal, e.g., light and heavy hole states)

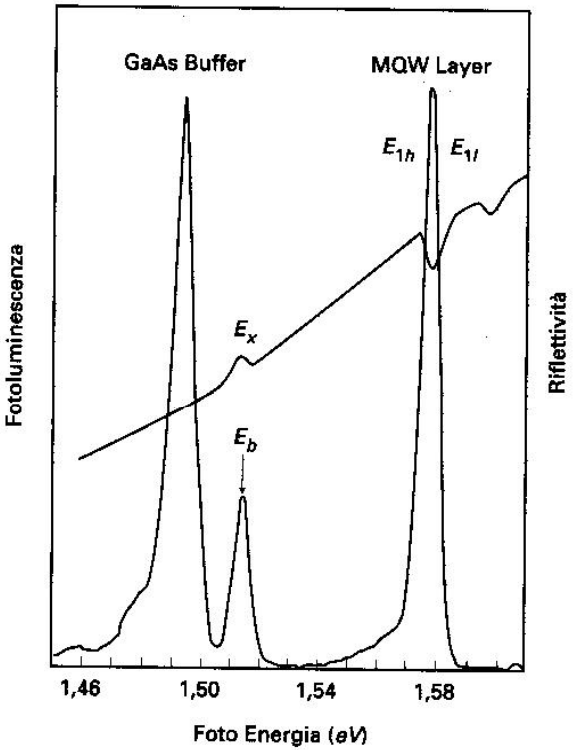

Figura 12.28
Fluorescenza eccitonica da un pozzo quantico (Q.W.) GaAs/$Ga_{1-x}Al_xAs$ e dal substrato GaAs a 12 K. E_b indica la posizione dell'eccitone nel substrato, E_{1h} ed E_{1l} gli eccitoni di buca pesante e di buca leggera nel Q.W. Per confronto è riportata anche la riflettività. Il picco di buca leggera compare soltanto ad alte temperature in fluorescenza, mentre è visibile in riflettività. (Da Y. Chen, R. Cingolani, L.C. Andreani, F. Bassani e J. Massies, Il Nuovo Cimento **D10**, 847 (1988)).

Minibands in MQW

A superlattice is formed by a periodic array of quantum structures (quantum wells, quantum wires, and quantum dots). An example of such a superlattice is a multiple quantum well, produced by growth of alternate layers of a wider bandgap (e.g., AlGaAs) and a narrower bandgap (GaAs) semiconductors in the growth (confinement) direction. This type of multiple quantum wells is shown in Figure 4.10a,b by a schematic of their spatial arrangement as well as by a periodic variation of their conduction and valence band edges.

When these quantum wells are widely separated so that the wavefunctions of the electrons and the holes remain confined within individual wells, they can be treated as a set of isolated quantum wells. In this case, the electrons (or the holes) can not tunnel from one well to another. The energies and wavefunctions of electrons (and holes) in each well remain unchanged even in the multiple quantum well arrangement. However, such noninteracting multiple quantum wells (or simply labeled multiple quantum wells) are often utilized to enhance an optical signal (absorption or emission) obtainable from a single well. An example is lasing, to be discussed in the next section, where the stimulated emission is amplified by traversing through multiple quantum wells, each well acting as an independent medium.

To understand the interaction among the quantum wells, one can use a perturbation theory approach similar to treating identical interacting particles with degenerate energy states. As an example, let us take two quantum wells separated by a large distance. At this large separation, each well has a set of quantized levels E_n labeled by quantum numbers $n = 1, 2, \ldots$ along the confinement direction (growth direction). As the two wells are brought close together so that the interaction between them becomes possible, the same energy states E_n of the two wells are no longer degenerate. Two new states E_n^+ and E_n^- result from the symmetric (positive) overlap and antisymmetric (negative) overlap of the wavefunctions of the well. The $E_n^+ = E_n + \Delta_n$ and $E_n^- = E_n - \Delta_n$ are split by twice the interaction parameter Δ_n for level n.

The magnitude of the splitting, $2\Delta_n$, is dependent on the level E_n. It is larger for higher energy levels because the higher the value of n (the higher the energy value E_n), the more the wavefunction extends in the energy barrier region allowing more interaction between the wells.

The case of two wells now can be generalized into the case of N wells. Their interactions lift the energy degeneracy to produce splitting into N levels, which are closely spaced to form a band, the so-called miniband. In an infinite multiple quantum well limit, the width of such a miniband is $4\Delta_n$, where Δ_n is the interaction between two neighboring wells for the level n. This result is shown in Figure 4.11 for the two levels E_1 and E_2 for the case of a superlattice consisting of alternate layers of GaAs (well) and $Al_{0.11}Ga_{0.89}As$ (barrier), each of width 9 nm. For this system, the miniband energies are $E_1 = 26.6$ meV and $E_2 = 87$ meV, with the respective bandwidth of $\Delta E_1 = 2.3$ meV and $\Delta E_2 = 20.2$ meV (Barnham and Vvedensky, 2001). As explained above, the higher-energy miniband (E_2) has a greater bandwidth (ΔE_2) than the lower energy miniband (ΔE_1).

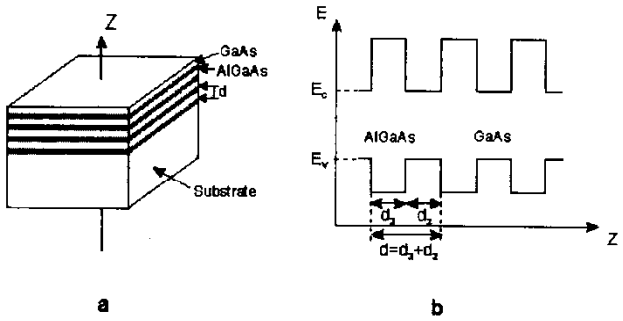

Figure 4.10. Schematics of the arrangement (a) and the energy bands (b) of multiple quantum wells.

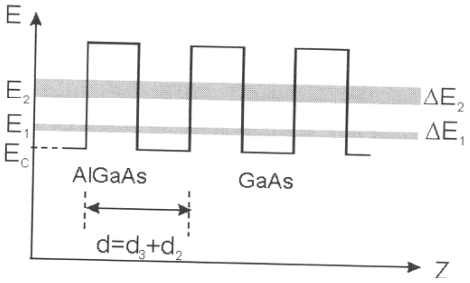

Figure 4.11. Schematics of formation of minibands in a superlattice consisting of alternate layers of GaAs (well) and AlGaAs (barrier).

- ✓ **"Minibands" formed due to interaction of different wells**
- ✓ **Consequences in QC lasers**

Electroluminescent systems: lasers (and LEDs)

Basic ingredients for a laser:
-**Active medium** (amplification through stimulated emission);
-**Optical cavity** (feedback of the active medium for coherent emission)

Note: *if cavity is missing, an incoherent emitting device (i.e., a LED) is obtained*

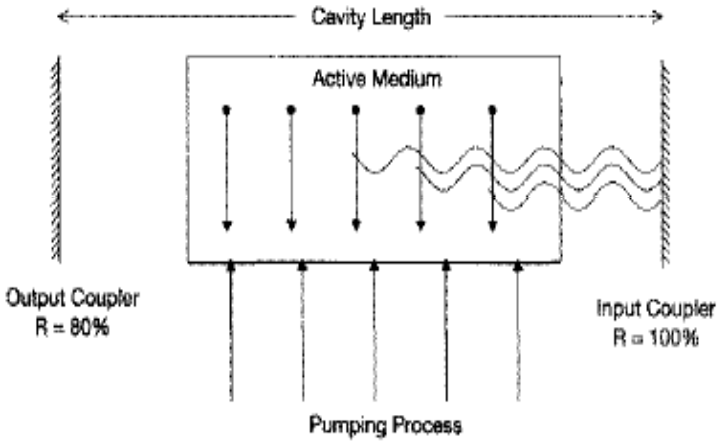

Figure 4.16. The schematics of a laser cavity. *R* represents percentage reflection.

In diode lasers (and LEDs) **pumping is achieved by electrical means**: current flow promotes electrons into the conduction band (and holes remain in the valence band) Electron/hole recombination leads to emission

Process is "enhanced" in the presence of excitons

If gain is large, couplers can be made of transitions between media having different refractive indexes (e.g., semiconductor/air)

"Conventional" diode lasers (with emission in a variety of spectral intervals) exploit quantum wells

Table 4.3. Quantum-Confined Semiconductors and the Lasing Wavelength Region

Quantum-Confined Active Layer	Barrier Layer	Substrate	Lasing Wavelength (nm)
InGaN	GaN	GaN	400–450
InGaP	InAlGaP	GaAs	630–650
GaAs	AlGaAs	GaAs	800–900
InGaAs	GaAs	GaAs	900–1000
InAsP	InGaAsP	InP	1060–1400
InGaAsP	InGaAsP	InP	1300–1550
InGaAs	InGaAsP	InP	1550
InGaAs	InP	InP	1550

The first diode laser (1962)

For Hall, who already had extensive experience with GaAs alloy junctions, tunnel diodes, and light-emitting diodes, the project to make a laser diode was an extension of his prior research work. It also coupled well with his optical experience in his earlier youthful hobbyist efforts to build telescopes and to polish lenses and mirrors [3]. Hall's laser project team included Dick Carlson, Gunther Fenner, Jack Kingsley, and Ted Soltys. Whereas other groups thinking about semiconductor lasers had proposed to use a macroscopic "external cavity" into which a GaAs diode was placed, Hall decided to polish parallel faces onto his GaAs diodes so that the Fabry- Perot optical cavity geometry was built into the device. This approach was not universally applied and, in fact, the importance of optical feedback into the diode "active region" was not fully appreciated by many workers. Hall's team operated their first successful GaAs laser diodes under pulsed conditions at 77K on September 16, 1962 [1]. A schematic diagram of Hall's early concept for an injection laser is shown in Figure 1. The first

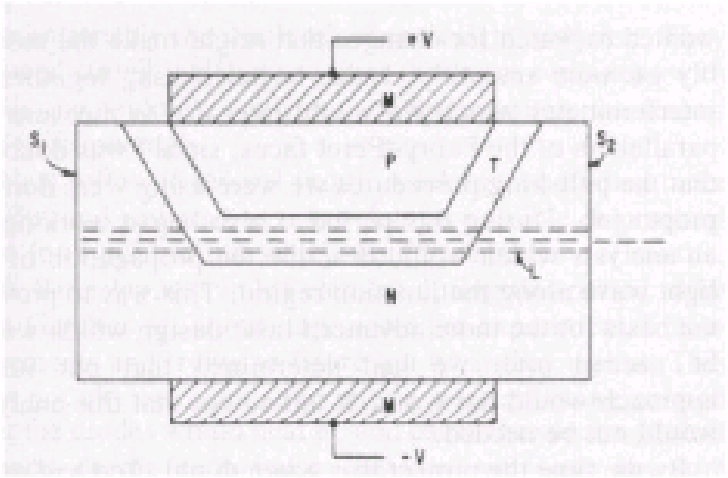

Figure 1: Schematic diagram of initial concept for an injection laser developed at General Electric Research Laboratories by Robert Hall in 1962.

© 1987/2000 IEEE

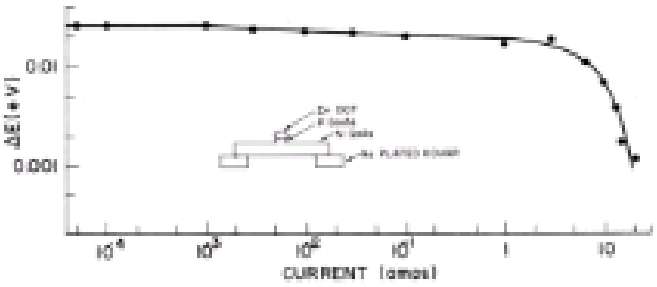

Figure 2: Spectral linewidth vs. current for a GaAs diode made at IBM and operated at 77K. The diode did not have a Fabry-Perot geometry so cavity modes were not observed.

© 1987/2000 IEEE

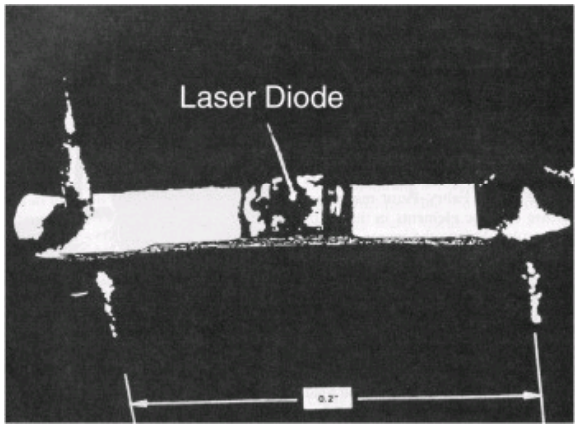

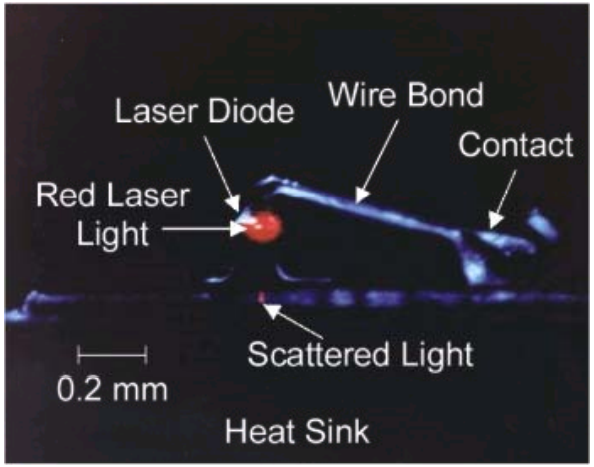

“Conventional” (heterojunction) diode laser

In the case of a semiconductor quantum well laser, the active medium is a narrow bandgap semiconductor (e.g., GaAs) that is sandwiched between a *p*-doped (excess holes) AlGaAs and an n-doped (excess electrons) AlGaAs barrier layer. However, in most semiconductor lasers, the doped layers of AlGaAs are separated from GaAs by a thin undoped layer of same composition AlGaAs. The cavity is formed by the cleaved crystal surfaces that act as reflectors. The general principle for the semiconductor lasers can be illustrated by the schematic shown in Figure 4.17 for a double heterostructure semiconductor laser. The ohmic contacts on the top and bottom inject electrons and holes into the active region, which in this design is significantly thicker (>100 nm) than a quantum well. The electrons and holes combine in the active region (GaAs in the present case) to emit a photon. The threshold current density (current per cross-sectional area) is defined as the current density required for the onset of stimulated emission and hence lasing. At this current density, the optical gain produced in the medium by stimulated emission just balances the optical loss due to various factors (e.g., scattering, absorption loss, etc.). A thick active layer in the double heterostructure also acts as a waveguide to confine the optical waves. The output emerges from the edges, hence this configuration is also referred to produce edge emitting laser action.

The case of a quantum well laser, where a single quantum well of dimensions <10 nm (depends on the material) is used as the active layer, is referred to as SQW (single quantum well) laser. This thickness is too small to confine the optical wave, which then leaks into the confining barrier region. To simultaneously confine the carriers in the quantum well and the optical wave around it, one uses a layer for optical confinement in which the quantum well is embedded.

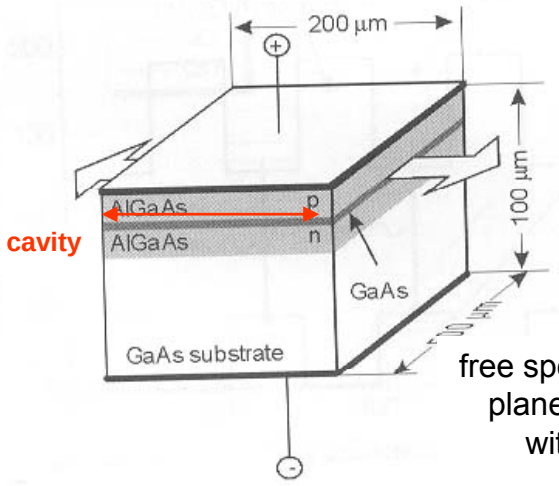

free spectral range for a plane-parallel cavity with length = L

$\Delta\nu = c/2L$

Figure 4.17. Scheme of double heterostructure semiconductor (DHS) lasc

MQW frequently used as the active medium in order to enhance amplification (and reduce the threshold current)

Conventional semiconductor laser:

Light is generated across material's band-gap

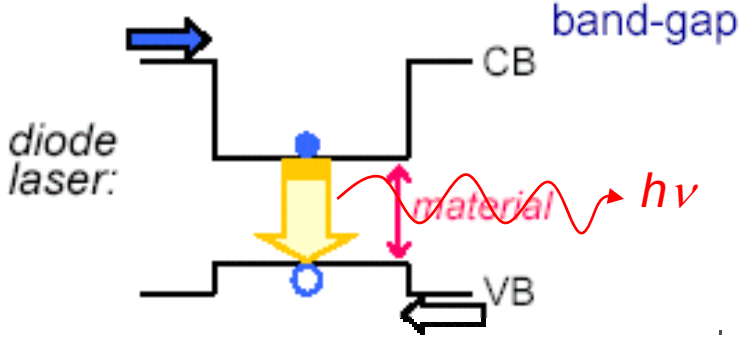

Market issues

Table 1. Worldwide commercial diode-laser sales 2004–2005 (units)

DIODE UNITS		Materials processing	Medical	Instrumentation	Basic research	Telecommunications	Optical storage	Entertainment	Image recording	Inspection, measurement, and control	Barcode scanning	Sensing	Other	Solid-state laser pumping	TOTALS
<700 nm	2004	50	800	200	0	0	274,500,000	43,000,000	15,000	13,630,000	5,700,000	0	0	0	336,846,050
	2005	100	1,000	300	0	0	341,700,000	43,000,000	17,250	13,660,000	6,300,000	0	0	0	404,678,750
750–980 nm <100 mW	2004	0	0	0	0	0	369,000,000	0	8,600,000	140,000	0	2,300,000	10,210,000	0	390,250,000
	2005	0	0	0	0	0	329,000,000	0	9,100,000	160,000	0	3,700,000	12,050,000	0	354,010,000
750–980 nm 100 mW–10 W	2004	1,250	147,000	600	0	55,000	0	0	93,125	0	0	0	1,000	107,000	404,975
	2005	1,475	162,000	900	0	65,000	0	0	82,500	0	0	0	1,2754	129,000	442,150
750–980 nm >10 W	2004	755	58,500	0	1,000	0	0	0	4,467	0	0	10,000	31,000	19,000	124,722
	2005	855	76,000	0	1,000	0	0	0	5,100	0	0	10,000	31,100	21,133	145,388
908–1550 nm	2004	0	500	0	0	3,622,500	0	0	0	0	0	0	1,536,500	0	5,159,500
	2005	0	500	0	0	4,827,500	0	0	0	0	0	0	1,812,500	0	6,639,500
>1550 nm	2004	0	0	0	0	0	0	0	0	0	0	0	0	0	0
	2005	0	0	0	0	0	0	0	0	0	0	0	0	0	0
Stacks	2004	500	3,250	0	50	0	0	0	0	0	0	0	200	8,250	12,250
	2005	672	3,000	0	50	0	0	0	0	0	0	0	300	9,000	13,022
TOTAL UNITS	2004	2,555	210,050	800	1,050	3,677,500	643,500,000	43,000,000	8,712,592	13,770,000	5,700,000	2,310,000	11,778,700	134,250	732,797,497
	2005	3,102	242,600	1,200	1,050	4,892,500	670,700,000	43,000,000	9,204,850	13,820,000	6,300,000	3,710,000	13,895,175	159,333	765,929,810

Huge figures, but there is still space for further progress

“Nanotechnological” diode lasers III: QC

Completely new approach to lasing action with the goals:
-Mid-IR lasers with possibility to engineer wavelength (e.g., for trace analysis);
-Huge efficiency (low threshold, high power)

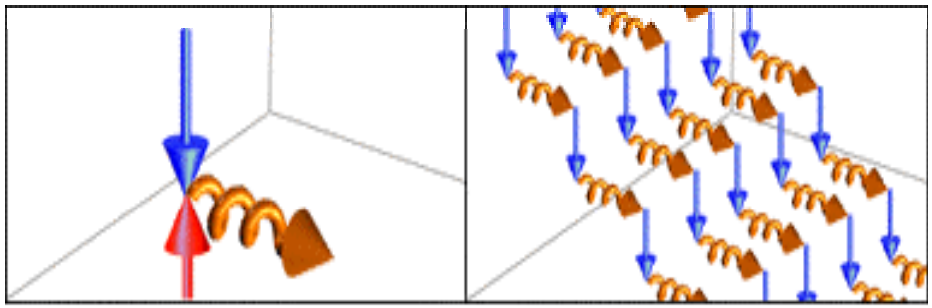

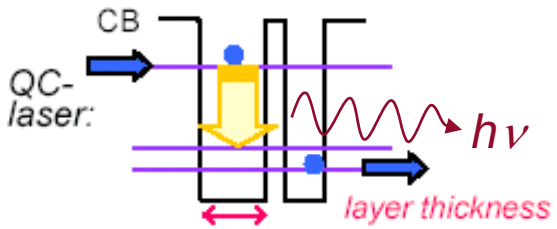

QC-laser:
Light is generated across designed energy ga
"materials by design":
band structure engineering and MBE

- In contrast to the lasers discussed above, which involve the recombination of an electron in the conduction band and a hole in the valence band, the QC lasers use only electrons in the conduction band. Hence they are also called unipolar lasers.
- Unlike the quantum-confined lasers discussed above, which involve an inter-band transition between the conduction band and the valence band, the QC lasers involve intraband (inter-sub-band) transition of electrons between the various sub-bands corresponding to different quantized levels of the conduction band. These sub-bands have been discussed in Section 4.1.
- In the conventional laser design, one electron at the most can emit one photon (quantum yield one). The QC lasers operate like a waterfall, where the electrons cascade down in a series of energy steps, emitting a photon at each step. Thus an electron can produce 25–75 photons.

See http://www.unine.ch/phys/meso

Quantum Cascade lasers I

Figure 4.21 illustrates the schematics of the basic design principle of an earlier version of the QC lasers that produce optical output at 4.65 μm. These lasers are based on AlInAs/GaInAs. It consists of electron injectors comprised of a quantum well superlattice in which each quantized level along the confinement is spread into a miniband by the interaction between wells, which have ultrathin (1–3 nm) barrier layers. The active region is where the electron makes a transition from a higher sub-band to a lower sub-band, producing lasing action. The electrons are injected from left to right by the application of an electric field of 70 kV/cm as shown in the slope diagram. Under this field, electrons are injected from the ground state *g* of the miniband of the injector to the upper level 3 of the active region. The thinnest well in the active region next to the injector facilitates electron tunneling from the injector into the upper level in the active region. The laser transition, represented by the wiggly arrow, occurs between levels 3 and 2, because there are more electron populations in level 3 than in level 2. The composition and the thickness of the wells in the active region are judiciously manipulated so that level 2 electron relaxes quickly to level 1.

The cascading process can continue along the direction of growth to produce more photons. In order to prevent accumulation of electrons in level 1, the exit barrier of the active region is, again, made thin, which allows rapid tunneling of electrons into a miniband of the adjacent injector. After relaxing into the ground state *g* of the injector, the electrons are re-injected into the next active region. Each successive active region is at a lower energy than the one before; thus the active regions act as steps in a staircase. Therefore, the active regions and the injectors are engineered to allow the electrons to move efficiently from the top of the staircase to the

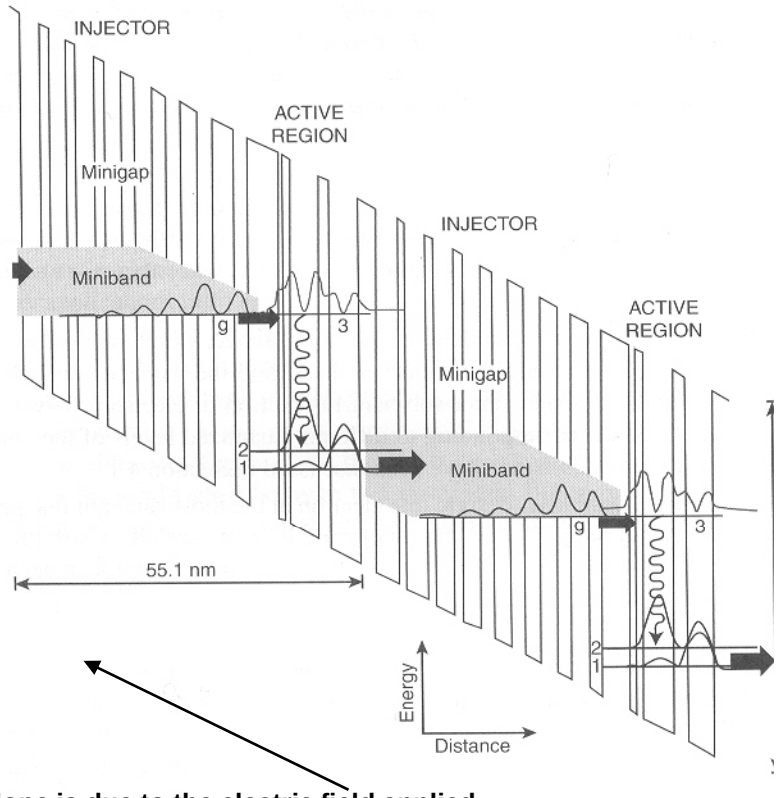

The slope is due to the electric field applied

Careful engineering and manufacturing of electron injector and active layers allow to achieve an efficient cascade behavior

Quantum Dots and photoluminescence

4.1.3 Quantum Dots

Quantum dots represent the case of three-dimensional confinement, hence the case of an electron confined in a three-dimentional quantum box, typically of dimensions ranging from nanometers to tens of nanometors. These dimensions are smaller than the de Broglie wavelength thermal electrons. A 10-nm cube of GaAs would contain about 40,000 atoms. A quantum dot is often described as an artificial atom because the electron is dimensionally confined just like in an atom (where an electron is confined near the nucleus) and similarly has only discrete energy levels. The electrons in a quantum dot represent a zero-dimensional electron gas (0DEG). The quantum dot represents a widely investigated group of confined structures with many structural variations to offer. The size dependence of the lower excited electronic state of semiconductor nanocrystals has been a subject of extensive investigation for a long time (Brus, 1984). Quantum dots of all types of semiconductors listed in Table 4.1 have been made. Also, as we shall see in Chapter 7, a wide variety of methods have been utilized to produce quantum dots. Recent efforts have also focused on producing quantum dots in different geometric shapes to control the shapes of the potential barrier confining the electrons (and the holes) (Williamson, 2002).

A simple case of a quantum dot is a box of dimensions l_x, l_y, and l_z. The energy levels for an electron in such a case have only discrete values given as

$$E_n = \frac{h^2}{8m_e}\left[\left(\frac{n_x}{l_x}\right)^2 + \left(\frac{n_y}{l_y}\right)^2 + \left(\frac{n_z}{l_z}\right)^2\right] \quad (4.7)$$

Energy

where the quantum numbers l_x, l_y, and l_z, each assuming the integral values 1, 2, 3, characterize quantization along the x, y, and z axes, respectively. Consequently, the density of states for a zero-dimensional electron gas (for a quantum dot) is a series of δ functions (sharp peaks) at each of the allowed confinement state energies.

$$D(E) \propto \sum_{E_n} \delta(E - E_n) \quad (4.8)$$

0-DEG DOS

In other words, $D(E)$ has discrete (nonzero) values only at the discrete energies given by Eq. (4.8). This behavior for $D(E)$ is also shown in Figure 4.3. The discrete values of $D(E)$ produce sharp absorption and emission spectra for quantum dots, even at room temperature. However, it should be noted that this is idealized, and the singularities are often removed by inhomogeneous and homogeneous broadening of spectroscopic transitions (see Chapter 6).

Another important aspect of a quantum dot is its large surface-to-volume ratio of the atoms, which can vary as much as 20%. An important consequence of this feature is strong manifestation of surface-related phenomena.

Quantum dots are often described in terms of the degree of confinement. The strong confinement regime is defined to represent the case when the size of the quantum dot (e.g., the radius R of a spherical dot) is smaller than the exciton Bohr radius a_B. In this case, the energy separation between the sub-bands (various quantized levels of electrons and holes) is much larger than the exciton binding energy. Hence, the electrons and holes are largely represented by the energy states of their respective sub-bands. As the quantum dot size increases, the energy separation between the various sub-bands becomes comparable to and eventually less than the exciton binding energy. The latter represents the case of a weak confinement regime where the size of the quantum dot is much larger than the exciton Bohr radius. The electron–hole binding energy in this case is nearly the same as in the bulk semiconductor.

Table 4.1. Semiconductor Material Parameters

Material	Periodic Table Classification	Bandgap Energy (eV)	Bandgap Wavelength (μm)	Exciton Bohr Radius (nm)	Exciton Binding Energy (meV)
CuCl	I–VII	3.395	0.36	0.7	190
CdS	II–VI	2.583	0.48	2.8	29
CdSe	II–VI	1.89	0.67	4.9	16
GaN	III–V	3.42	0.36	2.8	
GaP	III–V	2.26	0.55	10–6.5	13–20
InP	III–V	1.35	0.92	11.3	5.1
GaAs	III–V	1.42	0.87	12.5	5
AlAs	III–V	2.16	0.57	4.2	17
Si	IV	1.11	1.15	4.3	15
Ge	IV	0.66	1.88	25	3.6
$Si_{1-x}Ge_x$	IV	$1.15–0.874x + 0.376x^2$	$1.08–1.42x + 3.3x^2$	$0.85–0.54x + 0.6x^2$	$14.5–22x + 20x^2$
PbS	IV–VI	0.41	3	18	4.7
AlN	III–V	6.026	0.2	1.96	80

Important photoluminescence features in quantum dots

NC in colloidal solutions

CdSe nanocrystals in solution

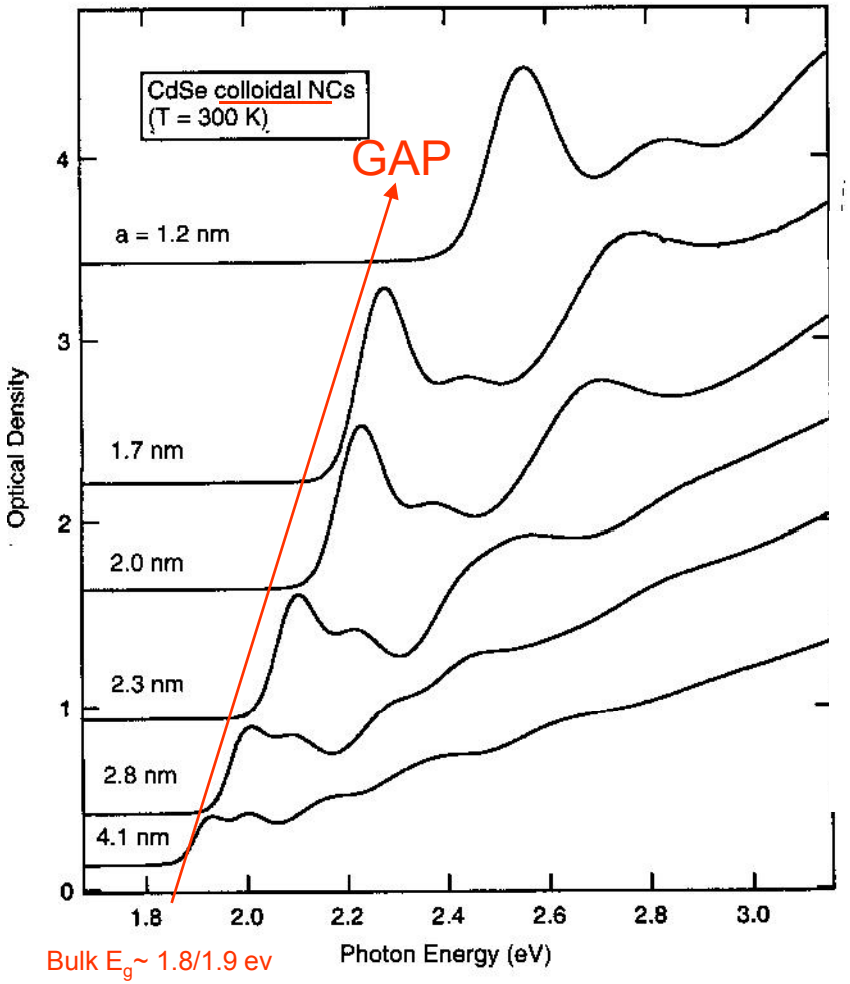

Bulk E_g~ 1.8/1.9 ev

ure 3.27. Room-temperature optical absorption spectra for CdSe colloidal nanocrystals
Cs) with mean radii in the range from 1.2 to 4.1 nm. [From V. I. Klimov, in Nalwa (2000),
l. 4, Chapter 7, p. 464.]

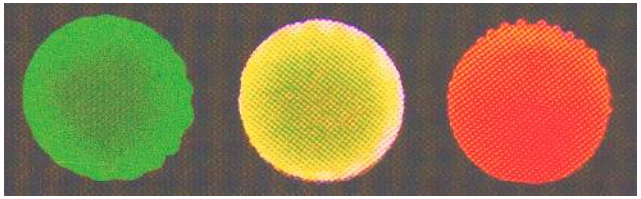

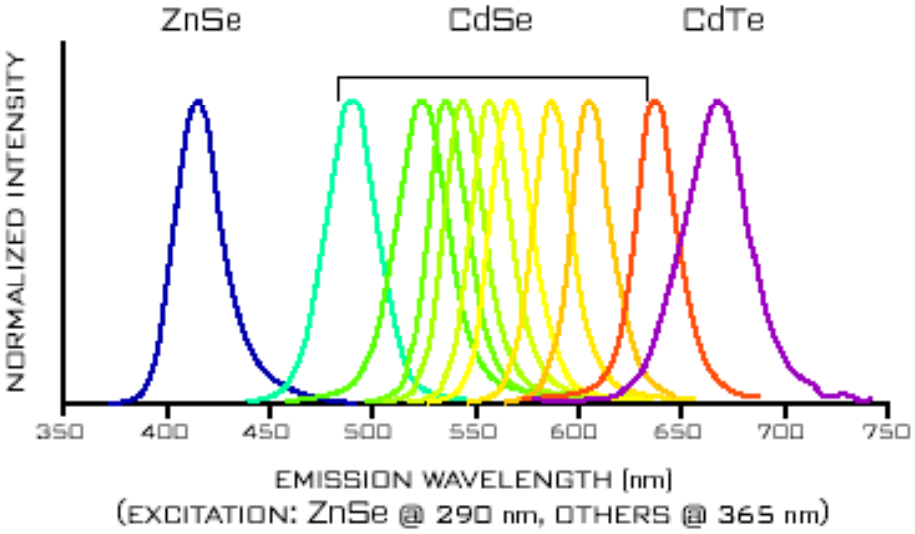

Wide "tunability" of PL range

C.P.Poole F.J.Owens
Introd. to Nanotechnology
(Wiley, 2003)

QDs nanoislands on surfaces

AFM images

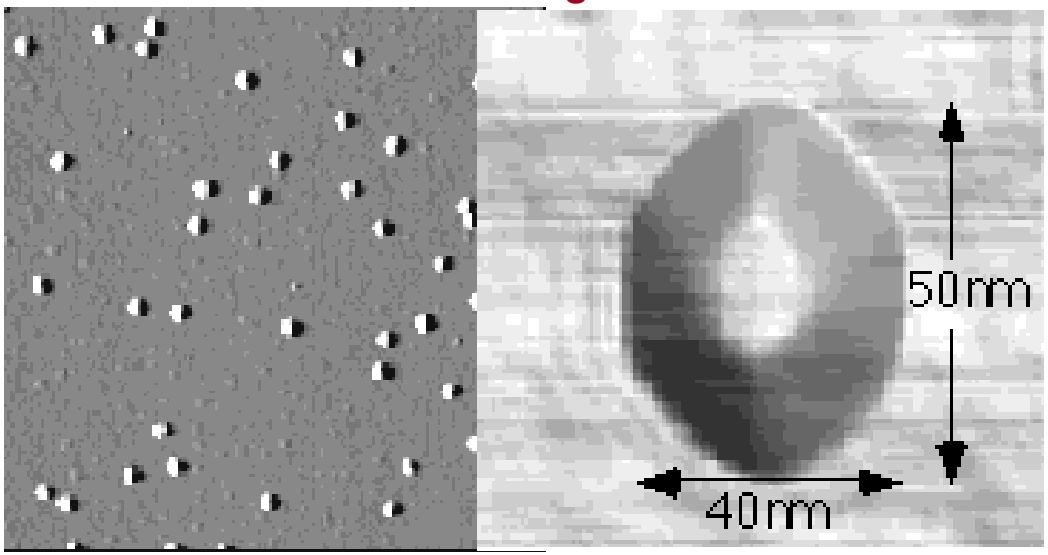

InP islands grown on and capped with InGaP (fabricated via MetallOrganic VaporPhaseEpitaxy)

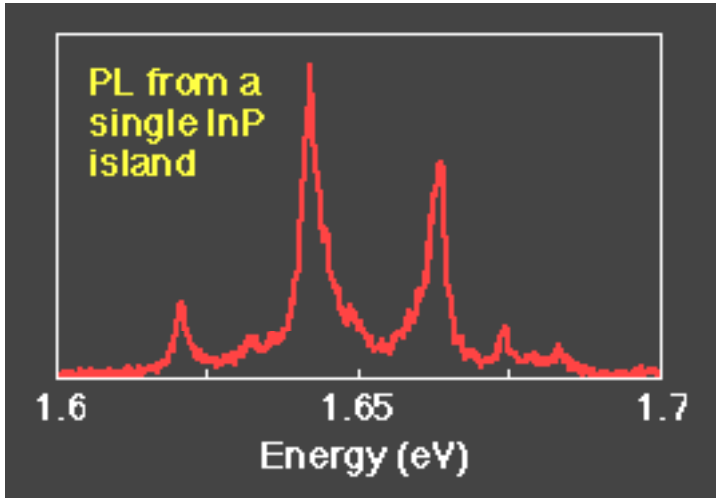

Spectral signatures of excitonic behavior:
sharp and strong PL (observed at room temp)

See Hessmann et al. APL 68 (1996)

Bulk E_g~ 1.5 ev

Core/shell Quantum Dots

This section describes semiconductor nanostructures that consist of a quantum dot core with one or more overlayers of a wider bandgap semiconductor. The core-shell quantum dots consist of a quantum dot with one overcoating (shell) of a wider bandgap semiconductor (Wilson et al., 1993; Hines and GuyotSionnest, 1996). The quantum dot–quantum well (QDQW) structure involves an onion-like nanostructure composed of a quantum dot core surrounded by two or more shells of alternating lower and higher bandgap materials (Schooss et al., 1994). These types of hierarchical nanostructures introduce a new dimension to bandgap engineering (modifications of the bandgap profile, charge-carrier properties, and luminescence feature). In the case of a core-shell structure, changing the shell can be used to manipulate the nature of carrier confinement in the core, thus affecting the optical properties. Furthermore, an overcoating with a wider bandgap semiconductor passivates the surface nonradiative recombination sites, thereby improving the luminescence efficiency of the quantum dot. In the case of QDQW structures, additional tuning of the energy levels and carrier wavefunctions can be obtained by varying the nature and the width of the quantum well surrounding the quantum dot.

Numerous reports of core-shell quantum dots exist. Some examples are ZnS (shell) on CdSe (quantum dots) (Dabbousi et al., 1997; Ebenstein et al., 2002), CdS on CdSe (Tian et al., 1996; Peng et al., 1997), ZnS on InP (Haubold et al., 2001), and $ZnCdSe_2$ on InP (Micic et al., 2000). The use of a wider bandgap semiconductor shell permits the light emitted from the core quantum dot to be transmitted through it without any absorption in the shell. These core-shell structures exhibit many interesting modifications of their luminescence properties. As an example, the results reported by Dabbousi et al. for the CdSe–ZnS core-shell quantum dots are summarized below:

- A small red shift in the absorption spectra of the core-shell quantum dot compared to that for the bare quantum dot is observed. This red shift is explained to arise from a partial leakage of the electronic wave function into the shell semiconductor. When a ZnS shell surrounds the CdSe quantum dot, the electron wavefunction is spread into the shell but the hole wavefunction remains localized in the quantum dot core. This effect produces a lowering of the bandgap and consequently a red shift. The red shift becomes smaller when the difference between the bandgaps of the core and the shell semiconductor increases. Hence, a CdSe–CdS core-shell structure exhibits a large red shift compared to the bare CdSe quantum dot of the same size (CdSe core). Also, the red shift is more pronounced for a smaller-size quantum dot where the spread of the electronic wavefunction to the shell structure is increased.
- For the same size CdSe quantum dot (~4 nm), as the coverage of the ZnS overlayer increases, the photoluminescence spectra show an increased red shift of emission peak compared to the absorption peak, with an increase in broadening. This effect may arise from an inhomogeneous distribution of the size and preferential absorption into larger dots. The photoluminescence quantum yield first increases with the ZnS coverage reaching to 50% at approximately ~1.3 monolayer coverage. At higher coverage, it begins to decrease. The increase in the quantum yield is explained to result from passivation of surface vacancies and nonradiative recombination sites. The decrease at higher coverage was suggested to arise from defects in the ZnS shell producing new nonradiative recombination sites.

The reported core-shell structure fabrication methods have utilized procedures for formation of the core (quantum dots) which produce polydispersed samples of core nanoparticles. These core particles then must be size-selectively precipitated before overcoating, making the process inefficient and time-consuming.

More recently, we developed a rapid wet chemical approach to produce core-shell structures using novel chemical precursors which allows us to make III–V quantum dots (a more difficult task than the preparation of II–VI quantum dots) rapidly, (less than two hours) (Lucey and Prasad, 2003). Then without the use of surfactants or coordinating ligands, the quantum dots are overcoated by the shells rapidly using inexpensive and commercially available II–VI precursors that are not air-sensitive. This process was used to produce CdS on InP, CdSe on InP, ZnS on InP, and ZnSe on InP. The optical properties of these core-shell structures were strongly dependent on the nature of the shell around InP. A ZnS shell around the

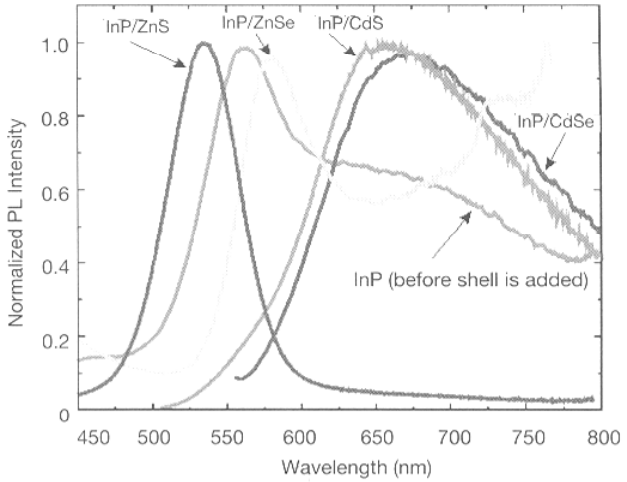

Figure 4.14. Photoluminescence spectra of InP quantum dots and the various core-shell structures involving InP core of some diameter (~3 nm).

Functionalization of core/shell QDs

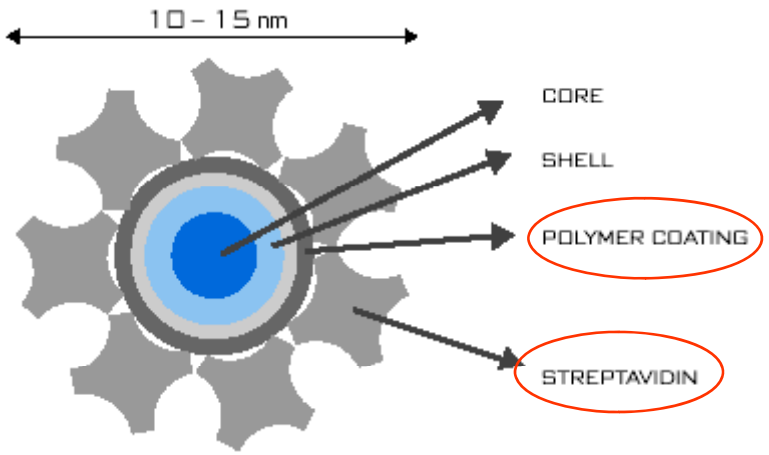

http://faculty.washington.edu/stenkamp/strep.html

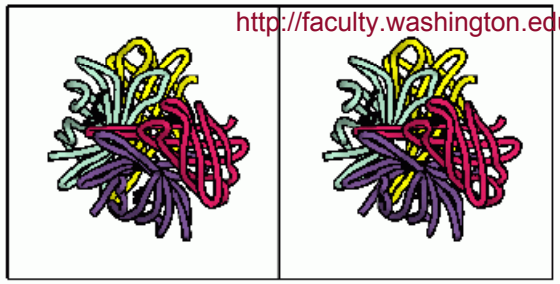

See www.qdots.com

Above is a stereoview of the streptavidin tetramer showing the subunit arrangement and the biotin binding site.

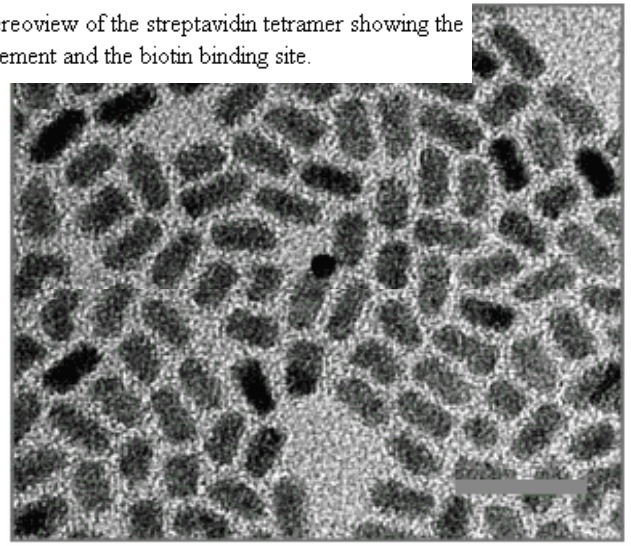

Electron Micrograph. Transmission electron microscopy can be used to directly image Qdot core-shell nanocrystals. The darker regions are the crystallites. Like several of QDC's products, these core-shell nanocrystals are rod-like in structure. The magnification is 200,000 and the scale bar is 20 nm.

Preparazione:
Core (CdSe)
$Cd(CH_3)_2$ e Se in TBP o TOP
reazione a 360°C e raffreddata 290°C, temp ambiente
controllo crescita tramite spettro di assorbimento
Shell (ZnS)
$(TMS)_2S$ e $Zn(Et)_2$ in TOP
reazione a 190°C
controllo crescita spettroscopia UV-Vis e fotoluminscenza

The shell can be further functionalized in order to be compatible with organics

Materiale tratto dal seminario di Marco Cirillo, Apr. 2004

Fluorescence marker applications

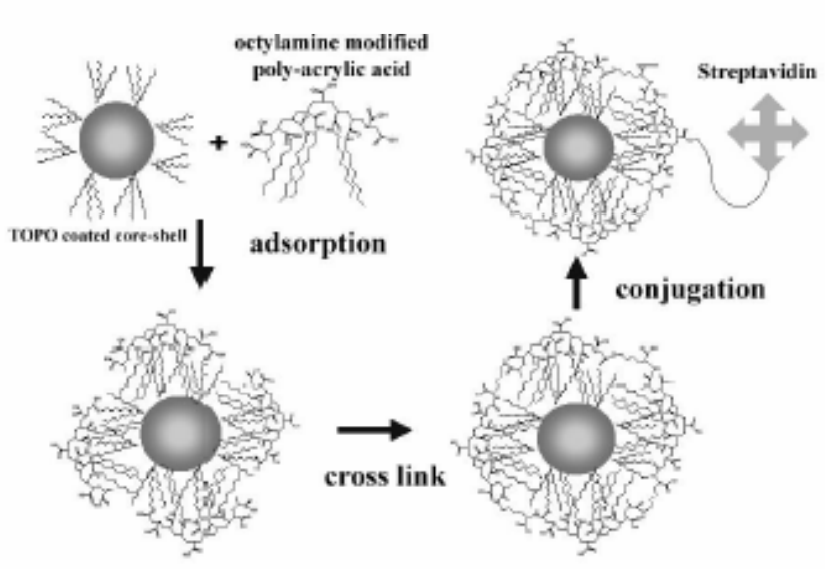

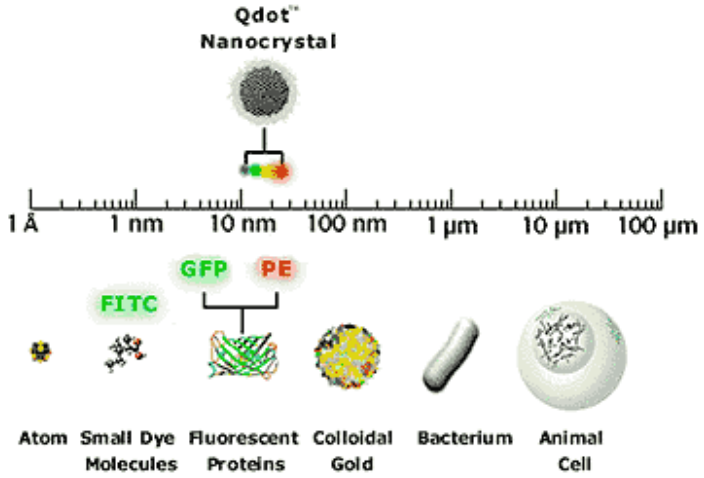

QDs preferred to molecular dyes for:
-Larger quantum efficiency;
-Larger "compatibility";
-High degree of versatility

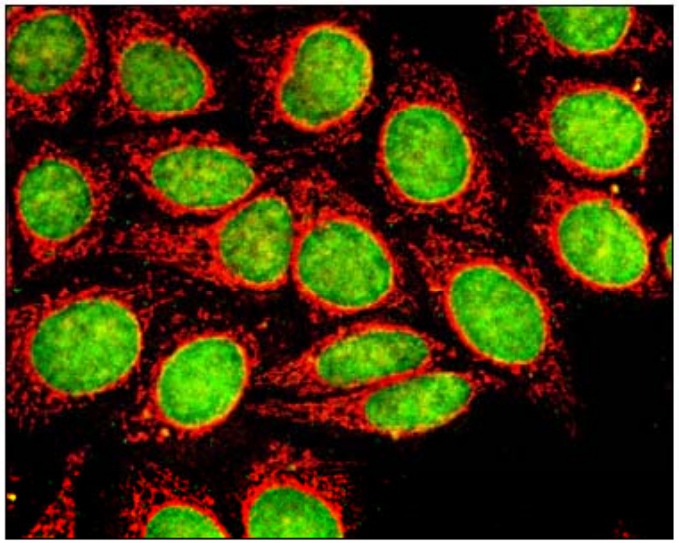

See www.qdots.com

Figure 1. Fluorescent double-labeling with Qdot Streptavidin Conjugates. Fixed human epithelial cells were incubated with a mixture of human anti-mitochondria antibodies and mouse anti-histone antibody. The mitochondria were labeled with Qdot 605 Streptavidin Conjugate (red) after the specimens were incubated with biotinylated goat anti-human IgG. The cells then were blocked with biotin solution, incubated with biotinylated goat anti-mouse IgG and the nuclei were stained with Qdot 525 Streptavidin Conjugate (green).

Conclusions

- ✓ Quantum physics (i.e., the semiclassical approach) offers a viable handle to understand many properties of matter depending on the electronic wavefunctions
- ✓ Despite of the (often complicated) details, the optical properties of semiconductors can be understood based on simple (energy balance) considerations, involving interband transitions of electrons
- ✓ However, practaical exploitations are often hampered by the actual arrangement of the energy levels (especially in Siilicon)
- ✓ Technology invented the way to assemble “artificial” semiconductors with the required band-gaps (and efficient transitions)
- ✓ Diode lasers (and LEDs) are typically based on those materials
- ✓ The same technology can be also used in a completely different field, where light-stimulated emission (photoluminescence) is required, e.g., fluorescence markers